HEFAT2014
10th International Conference on Heat Transfer, Fluid Mechanics and Thermodynamics
14 – 16 July 2014
Orlando, Florida

NUMERICAL STUDY OF NATURAL CONVECTION BOILING IN A PARTIALLY HEATED RAYLEIGH-BÉNARD CELL

Tilak T. Chandratilleke* and Nima Nadim
*Author for correspondence
Department of Mechanical Engineering,
Curtin University,
Perth, 6101,
Australia.
E-mail: t.chandratilleke@curtin.edu.au

ABSTRACT

This paper presents a numerical investigation on Rayleigh-Bénard (RB) cell with natural convective liquid boiling, which is vastly different to thermo-fluids nature of its classic single phase counter-part. The study develops a simulation model and examines the unique fluid and thermal characteristics associated with this two-phase RB cell for a range of heater power. The boiling heat transfer curve is obtained covering single phase to boiling process within the RB cell while identifying its unique fluid features. Unlike cellular convective structures in single-phase RB cell, the analysis on this boiling RB cell indicates a fast rising fluid plume emulating "siphoning" fluid action that develops according to heating levels and vapour composition. It also shows that the vapour bubble dynamics critically influence and determine vapour migration within the boiling fluid and heater surface thermal patterns, making this cell behaviour uniquely different to that of traditional RB cell and conventional pool boiling.

INTRODUCTION

Rayleigh-Bénard (RB) cell is a classic natural convective flow formation due to thermally-induced buoyancy arising from differential heating at the bottom and top (or sides) surfaces of a stagnant fluid mass. This kind of circulatory flow behaviour is commonly encountered in the large-scale geophysical [1] and astrophysical [2] flows such as atmosphere and oceans, where technological possibilities exist for sustainable energy harvesting. Such power generating systems make use of self-induced fluid circulation without relying on external pumping power for enhanced overall thermal plant efficiency. In view of practical significance, Rayleigh-Bénard cell behaviour has been a subject for widely pursued research in developing accurate understanding of its local boundary layer plume instability and associated heat transfer processes.

Literature reports numerous experimental and numerical investigations on RB cell characteristics involving a variety of geometrical, thermal and material combinations. Such analyses are largely limited to single phase fluids for its relatively simple flow processes compared to multi-phase domains. Nucleate boiling compounds the complexities of RB cell flow behaviour because of the evaporative and quenching phase change mechanisms present within the flow. Nonetheless, such multi-phase heat transfer processes offer much higher energy transfer potential than single phase systems and are set to deliver significant thermal benefits for power generating systems.

In multi-phase modelling applications, the Lagrangian schemes is generally utilised with dispersed gas phase assumption on which vapour volume fraction essentially limits its practical validity. The work of Lakkaraju [3] studied RB boiling cell in bubbly flow regime where small vapour bubbles assumed as dispersed phase with a model based on Lagrangian frame. Whilst this assumption is acceptable for resolving fine turbulence structures [highly resolved DPM] and permits understanding of fluid features for low void fractions, the model breakdowns for high values of void fractions. RPI model [4-7] is another highly established option for boiling models, where wall heat flux partitioning function is incorporated to the Eulerian multi-phase model.

This paper describes an investigation where an improved numerical methodology is developed and a parametric study is performed for accurate description of the multi-phase heat and fluid flow behaviour in RB cell. The application of existing multi-phase models to the RB boiling cell in the current study requires careful evaluation of momentum, phase and thermal exchange terms within the domain under several flow regimes arising from varying heat flux levels. Based on the model closures proposed by Podowski et al. [4], the current RB Cell simulation is developed by modifications to account for bubble dynamics, in particular bubble departure frequency (BDF), in accommodating the motion due to pure buoyancy and the coupled buoyancy-convective driven flow within the RB Cell. In addition, the momentum exchange properties are amended to account for higher void fraction beyond the validity limits of dispersed phase assumption.

NOMENCLATURE

C_d	[-]	Drag coefficient
C_p	J/kgK	Specific heat
D_w	M	Bubble departure diameter
f	Hz	Bubble departure frequency
$\vec{F}_{lift}$	N	Lift force
$\vec{F}^{TD}$	N	Turbulence drift force
$\vec{F}_{wl}$	N	Wall lubrication force
g	m/s^2	Gravity
h_{lg}	kJ/kg	Latent heat
k	m^2/s^2	Turbulent kinetic energy
$\dot{m}$	kg/s	Mass flux
p	Pa	Pressure
$\dot{q}$	W/m^2	Heat flux
r_c	M	Cavity radius
T	K	Temperature
u^*	m/s	Frictional velocity on the wall
v	m/s	Velocity
$\nabla\vec{V}$		Mean strain rate tensor
$\nabla\vec{V}^T$		Turbulent strain rate tensor
v^+	[-]	Dimensionless distance from wall
Subscripts		
E		Evaporative
L		Liquid
m		Mixture
p		Primary phase
q		Secondary phase
Q		Quenching
Sat		Saturation
Sub		Subcooled
Sup		Superheated
v		Vapour
w		Wall
Greek Symbols		
α		Volume fraction
μ	kg/ms	viscosity
ρ	kg/m^3	Density
σ	n/m	Surface tension coefficient
$\bar{\tau}$		Stress tensor
τ_D	s	Bubble dwelling time
τ_G	S	Bubble growth time
ω	1/s	Specific dissipation rate
λ	$k/\rho c_p$	Thermal diffusivity

PROBLEM DEFINITION, GEOMETRY AND BOUNDARY CONDITIONS

The numerical model used in the analysis is schematically shown in Figure 1. It consists of a cubic RB cell of 100 mm side length with a central heated area partially occupying the cell base, and a cooler top cell surface exposed to a convective ambient. The sides of the cell lose heat by convection to the surroundings at constant temperature. For a more realistic representation, the cell base heater of solid steel with 50 mm square and 0.5 mm thickness is considered to obtain uniformly distributed volumetric heating, which is adjustable from 20 to 100 MW/m^3. With this arrangement, a multi-phase conjugate heat transfer condition determines heat flux and temperature at the liquid-solid heater interface, instead of imposing thermal boundary conditions. To ensure liquid cooling, the top model surface is exposed to a convective ambient at $T_{Ref\text{-}Top}$ = 310 K with a heat transfer coefficient of h_{Top} = 20 W/m^2.K, while a heat transfer coefficient of h_{Side} = 5 W/m^2.K and a reference temperature $T_{Ref\text{-}Side}$=320 K are applied on the cell side walls. The applied heat generation is adjusted to investigate the thermal and flow behaviour from the initial single phase natural convection up to just before the onset of nucleate boiling (ONB), then through to nucleation boiling up to the critical heat flux (CHF) conditions.

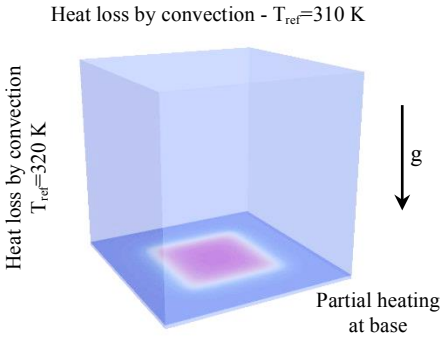

Fig. 1 Rayleigh-Bénard cell model with its partially heated base area and other boundary conditions

NUMERICAL METHOD: COMMON RPI FRAMEWORK AND FURTHUR IMPROVEMENTS

Traditional approach in RPI model consists of two key modelling elements-one to simulate multi-phase flow by incorporating drag, lift, interfacial mass and heat transfer, and the other to partition heating into averaged components, associated with various boiling stages. Eulerian framework uses independent sets of mass and momentum conservation equations per phase. Hence, continuity equation is given by,

$$\nabla(\alpha_q\rho_q\vec{v}_q) = \dot{m}_{qp} - \dot{m}_{pq} \quad (1)$$

This diffusive equation of volume fraction is used to track interface, where "p" and "q" denote primary (water) and secondary (vapour) phases. The mass transfer terms (on right hand side of Equation 1) account for simultaneous evaporation and condensation processes at vapour/liquid interfaces. Similarly, momentum equation is defined per phase as:

$$\nabla(\alpha_q\rho_q\vec{v}_q\vec{v}_q) = -\alpha_q\nabla p + \nabla\bar{\bar{\tau}}_q + \alpha_q\rho_q\vec{g} \quad (2)$$
$$+K_{pq}(\vec{v}_p - \vec{v}_q) + \dot{m}_{pq}\vec{v}_{pq} - \dot{m}_{qp}\vec{v}_{qp} + \vec{F}_q^{TD} + \vec{F}_{wl} + \vec{F}_{lift}$$

The terms for momentum exchange by drag, lift, mass transfer, wall lubrication force, turbulence dispersion in the general Eulerian equation of momentum are adjusted according

to the local boiling conditions. Turbulence and energy equations are solved for mixture domain, from which related scalars are recovered for each phase, according to the phase-to-mixture ratio of local properties. In consideration of wall heat transfer, k-ω SST turbulence closure, which is well adjusted for sub-layer solution, is applied in the model.

The current model is developed on a non-equilibrium base, which is a significant improvement over the established RPI approach. In this, heat transport in vapour phase is included to remove the weak temperature equilibrium assumption used in conventional RPI heat partitioning scheme. Nonetheless, all other RPI heat components (i.e. liquid convection, evaporation and quenching heat fluxes) are considered. Thus, the total externally applied heat flux at the heater surface is given by,

$$\dot{q}_{Total} = (\dot{q}_L + \dot{q}_Q + \dot{q}_E) f(\alpha) + \dot{q}_V [1 - f(\alpha)] \tag{3}$$

where $f(\alpha)$ is a smoothing function to accommodate various closures applicable to different flow regimes. All the empirical or mechanistic sub-models are derived from bubble dynamics, where bubble parameters are crucial for accuracy. Following critical parameters are considered: (a) Nucleation site density (N_w) to simulate bubble nucleation; (b) bubble diameter (D_w); and (c) bubble departure frequency ($f_{Departure}$).

From boiling RPI literature [5-7], the current model extracts common empirical correlation for nucleation site density and bubble departure diameter. However, it is realised that the Cole model [8] is inadequate for capturing physical phenomena involved in bubble departure frequency, thus an alternative option is used.

Nucleation site density is integrated through Lemmert and Chawala [9] equation as,

$$N_w = 210^{1.805} (T_w - T_{Sat})^{1.805} \tag{4}$$

whilst the bubble departure diameter is obtained by Tolubinski and Kostanchuk [10] correlation as,

$$D_w = \min(0.0014, 0.0006 \exp(-\frac{(T_{Sat} - T_b)}{45}) \tag{5}$$

In this, bulk temperature (T_b) is taken as liquid phase temperature, sufficiently far from the wall and to be physically outside of vapour jacket or departing bubble.

Cole [8] model has been widely applied for CFD boiling models as the trusted closure for bubble departure frequency, including pool and convective boiling situations. This model merely accounts for buoyancy force, correlated by density difference and bubble departure diameter. Yet, literature recognises the importance of additional parameters associated with velocity terms and surface characteristics affecting bubble departure frequency that is much critical for convective boiling than for pool boing. In the current study, the closure for bubble departure frequency is extracted from the Podowski [4] model since it considers a broad range of parameters for fluid ($T_{sat}, T_b, \lambda_l, k_l, h_{lv}, \rho_l, \rho_v, \sigma$) and solid heater ($T_w, \lambda_w, k_w, r_c,$).

Process of bubble evolution at boiling surface comprises a dwelling time and a growth time. During dwelling, a bubble grows until its radius reaches (micro-scale) cavity mouth size wherein quenching component of wall heat flux sustains growth. Following this, the bubble grows by evaporative heat flux component and departs having reached at a critical size. Podowski model accounts for these time scale (τ_D, τ_G) separately, and calculates departure frequency from, $f_{Departure} = \frac{1}{\tau_{B-Cycle}} = \frac{1}{\tau_D + \tau_G}$, whereas Cole [8] considers only τ_G .

Another key parameter needing enhancement is the drag force for estimating momentum exchange between liquid and vapour phases. Drag coefficient also indirectly affects interfacial heat and mass transfer. In boiling, drag coefficient depends on the two-phase flow regime and local vapour/liquid mixture composition. Both regime and composition display extreme changes when boiling undergoes transition from bubbly to slug and then to mist flow. Therefore, in a numerical scheme, the continuous phase will have to be altered from initial water (bubbly) to finally vapour (mist flow), and conversely, discrete bubbles (bubbly) to discrete droplets (mist flow). Void fraction is the only compatible criterion that recognises flow regime in Eulerian scheme with improved consistency of slip velocity between phases having high vapour content. Using this approach, the current model estimates drag from a function by Ishii and Zuber [11]. It distinguishes bubbly ($\alpha_v < 0.3$) and Churn turbulent flow ($0.3 < \alpha_v < 0.8$), where liquid is continuous phase, and mist flow regime ($\alpha_v > 0.8$) with vapour as continuous phase. Then, drag coefficient is obtained as,

$$C_D = \begin{cases} \frac{4}{6} D_b \sqrt{\frac{g\Delta\rho}{\sigma}} (1-\alpha_v)^{-0.5} & bubbly \\ \frac{8}{3} (1-\alpha_v)^2 & Churn \quad turbulent \\ \frac{4}{6} D_d \sqrt{\frac{g\Delta\rho}{\sigma}} (1-\alpha_l)^{-1.5} & mist \end{cases} \tag{6}$$

where, bubble (D_b) and droplet (D_d) diameters represent discrete particles dimensions in the core flow area of continuous phase. Unal's [12] formulation is used to calculate bubble diameter as,

$$D_b = \begin{cases} 0.0015 & \Delta T_{Sub} < 0 \\ 0.00015 - 0.0001 \Delta T_{Sub} & 0 < \Delta T_{Sub} < 13.5 \\ 0.00015 & \Delta T_{Sub} > 13.5 \end{cases} \tag{7}$$

Droplet (as dispersed particle) diameter in mist flow is estimated from a correlation by Kotaoka et al. [13] as,

$$D_d = 0.028 \frac{\sigma}{\rho_v V_v^2} \mathrm{Re}_l^{-1/6} \mathrm{Re}_v^{2/3} \left(\frac{\rho_v}{\rho_l}\right)^{-1/3} \left(\frac{\mu_v}{\mu_l}\right)^{2/3} \tag{8}$$

The essential interfacial source terms for completing the modelling framework are given in Table 1 with their associated physical phenomena.

Table.1 Boiling interfacial phenomena and applied closures

Source term	Model
Lift force	Morega et al. [14]
Turbulence dissipation	Lopez de Bertodano [15]
Turbulence agitation	Sato et al. [16]
Wall lubrication	Hosokawa et al. [17]
Heat transfer	Ranz-Marshal [18]

Whilst there are number of publications in literature covering boiling cases [5-7], such are for boiling with low void fraction and within narrow range. For this reason, a strict validation is not warranted. Nonetheless, the experimental boiling curve in Figure 6 provides an indirect prediction comparison in using Cole [8] and Podowski [4] models.

RESULTS AND DISCUSSION

This study of boiling Rayleigh-Bénard cell is performed with a specific interest on two key regions in the solution domain, namely in core fluid areas and at the heater surface. In the core fluid area, the analysis focusses on the thermally-driven flow and phase interaction, while over the heater surface, it examines the bubble behaviour and mechanisms of heat transfer. The results are presented and discussed as three typical cases: Case A for 20 MW/m^3; Case B for 60 MW/m^3; and Case C for 100 MW/m^3, based on volumetric heating.

(i) Siphonic flow

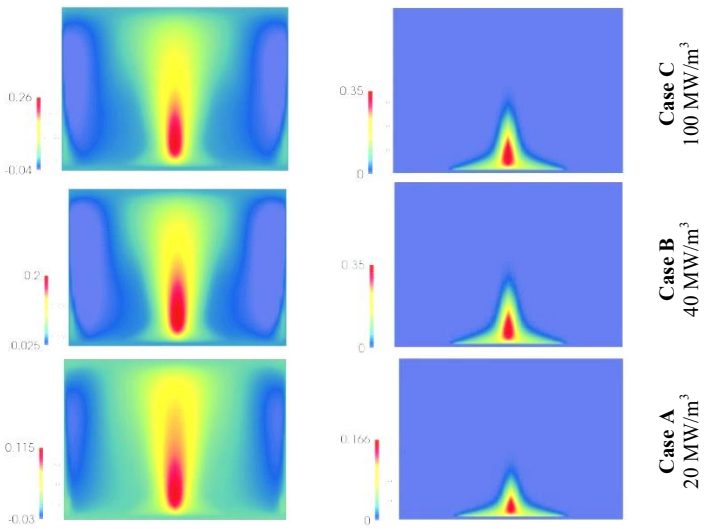

(a) Fluid velocity (m/s) *(b) Void fraction*

Fig. 2 Variation of fluid mixture velocity and vapour (void) fraction with heating over mid-plane of RB cell

Figure 2 illustrates typical profiles of (a) void (vapour) fraction distribution and (b) fluid velocity over the mid-plane of the RB cell. From Fig. 2(a), it is clearly evident that, the bottom heating induces a central upward fluid plume and a lateral fluid circulation over its periphery. This plume is essentially driven by buoyancy arising from the combined low densities of vapour bubbles and natural convection currents, thus much intense than such flow in single-phase RB cell with no bubbles. The lateral circulation, termed "siphonic effect", imparts significant flow velocities over the heater vicinity, making this RB cell behaviour uniquely different to that of its parallel single-phase situation.

Fig. 2(b) shows that the void fraction increases with higher heating levels resulting in more vapour bubble generation. The presence of large bubble population creates additional flow path resistance to impede the rising plume, thus reducing its discharging velocity. This behaviour is vindicated in Fig. 2(a), where the plume velocity declines as the heating is increased.

Vapour bubbles rising with the plume cool and condense while approaching the top of RB cell. With increased mixture density, the fluid then cascade down along the outer periphery of the RB cell, essentially sustaining the siphonic fluid motion and the overall flow circulation. This induced lateral fluid flow is initially almost non-existent and gradually intensifies with increased heating levels. Therefore within the RB cell, boiling begins in stagnant fluid (pool boiling) and then progressively transforms towards more of a flow (convective) boiling process. This transition intensifies if a wider temperature differential is applied between the top and the bottom of RB cell. It is envisaged that the critical heat flux (CHF) in this RB cell with base heating over partial area would significantly change from its value for traditional pool boiling.

These unique phase changing and flow characteristics bring about very high parametric gradients in velocity and temperature profiles in this RB solution domain. Bubble motion adds additional turbulence into the flow field. For these reasons, the RB cell with boiling exhibits more turbulent nature in the fluid medium that an equivalent single-phase cell. Hence, the model requires local mesh refinement while maintaining wall sublayer for consistency of heat transfer. In the solution domain, y^+ value was kept less than 5 in the implemented k-ω SST turbulence model while the flow intensity and (indirectly) the heat flux regulated the wall mesh refinement. Typically, in the heat generation range of 20 to 100 MW/m^3, mesh needed refinement of 17703 extra cells with intensifying Siphonic fluid action.

(ii) Bubble evolution

As a key influencing feature, bubble dynamics determines boiling heat transfer rates and phase interfacial exchanges. A single growing bubble initiates its life cycle in a micro-scale cavity (dwelling), grows attached to the heater surface while sliding and detaches to travel with the boiling liquid. Rising bubbles condense in subcooled regions of the liquid. Modelling schemes account for mass, momentum and heat transfer by averaging values over a single bubble life cycle, where a partitioning approach is used with empirical data. The current study incorporates such a correlation for bubble

diameter in core flow area to estimate the local drag force, interfacial area, bubble agitation, heat transfer and condensation rate. With increased heating, the boiling RB cell examined undergoes flow transitions from nearly pure buoyancy (pool boiling) to a combined action of buoyancy and advection (convective boiling). The current modelling accounts for this and computes the following results accordingly.

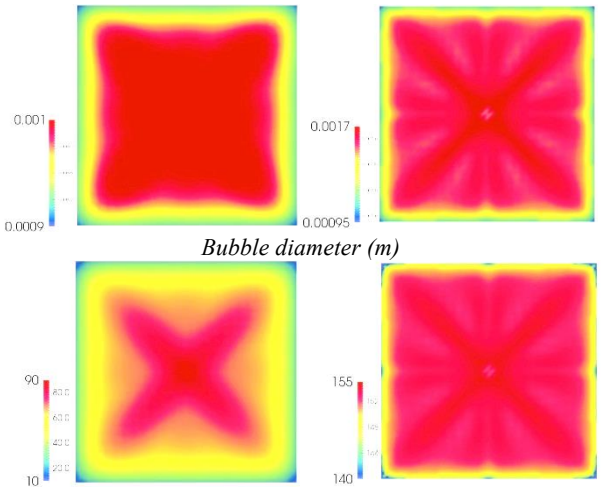

Bubble diameter (m)

Bubble departure frequency (Hz)

(a) Case A *(b) Case C*

Fig. 3 Bubble characteristics at the heater
(*Figure illustrates only the central heating area*)

Figure 3 shows bubble diameter and bubble departure frequency (BDF) at the heater for Case A and Case C with significantly different heating values. Between the two cases, the figure shows a more than 50% increase in bubble diameter and 60.5 to 151.9 Hz change in BDF. Also, the formation of larger bubbles and high departure frequencies seem to favour growth along the heater diagonals. These patterned behaviours are attributed to the siphonic flow characteristics that form low velocity regions broadly along the geometrical symmetry lines. Diagonal directions have the least velocities due to larger vertical flow circulatory path resistance and provide the bubbles with the fastest growth opportunity undisturbed by the siphonic flow and the highest BDF.

For a vertical diagonal plane passing through the centre of the heater, Figure 4 illustrates the variation of bubble diameter and vapour velocity starting from a point at the heater surface to the top cell boundary. During ascend, bubbles reduce in size due to condensation, while its velocity initially increases up to a peak and then drops off. This latter behaviour is caused by the lessening of bubble buoyancy (reduced size) and increased drag for bubble motion through the liquid. This mechanism essentially drives the siphonic fluid motion giving unique flow and thermal characteristics to the RB cell with boiling.

(iii) Boiling heat transfer

Effectiveness of boiling heat transfer is the prime interest of research investigations in view of thermally-optimised industry design whilst avoiding plant operation near the critical heat flux (CHF) region with burn-out possibility.

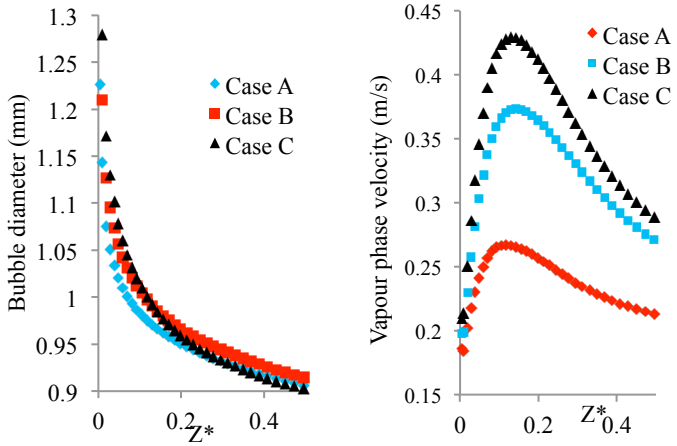

(a) Bubble diameter (b) Vapour velocity

Fig. 4 Bubble dynamics in the core flow area
(*Along vertical diagonal through centre of heater*)

Figure 5 provides the local values of void fraction and the wall/liquid superheat ($T\text{-}T_{sat}$) over the entire RB cell base. The void fraction and heater surface superheat temperature profiles show peak values along the heater diagonals. This is attributed to the flow formations created by the siphonic circulations, as described in relation to bubble size and departure frequency. These diagonal regions have the highest nucleation density, as reflected by large void fraction of which the maximum value jumps from 0.034 in Case A to 0.12 in Case C.

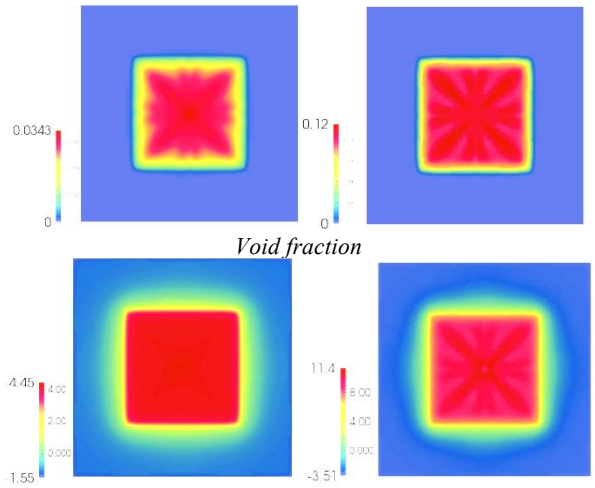

Void fraction

Superheat temperature, $T\text{-}T_{Sat}$ (°C)

(a) Case A *(b) Case C*

Fig. 5 Void fraction and superheat temperature at RB cell base
(*Heater depicted in the centre*)

The average heater wall superheat temperature indicates a 10 K increase between Case A and Case C. Unheated fluid region in line with the heater surface also shows a temperature increase due to lateral heat conduction and by advection (siphonic flow). Therefore, the overall heat delivery to the fluid has much enhanced effect than with single-phase RB Cell.

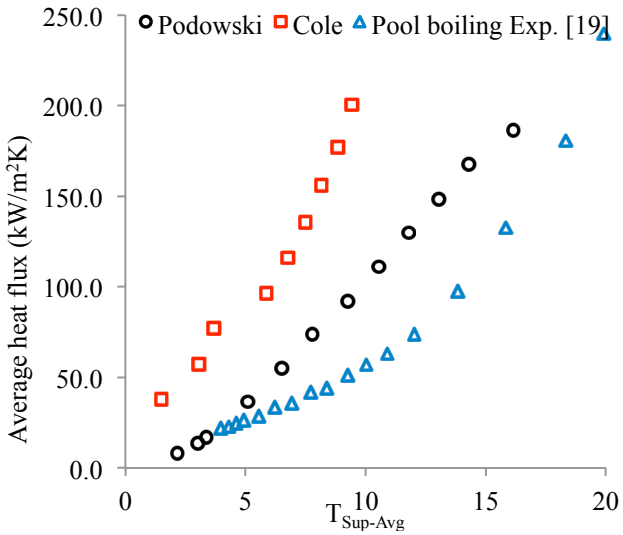

Fig. 6 Boiling curves - Rayleigh-Bénard vs. Pool boiling

Thermal effectiveness of RB boiling cell with its siphonic fluid action is depicted in Figure 6. This figure compares the current RB model predictions using both Podowski [4] and Cole [8] approaches for bubble dynamics, and the published pool boiling experimental data [12].

Cole BDF scheme [8] significantly over-predicts the results while the Podowski model [4] indicates slightly lower deviation from the experimental data. However, this latter prediction can be interpreted as boiling enhancement because the experimental data used are strictly for pure pool boiling where the siphonic fluid motion is not present.

CONCLUSIONS

This study presents a numerical investigation whereby Rayleigh-Bénard cell with boiling is successfully analysed. It identifies flow features uniquely characterising this RB cell due to the combined hydro-thermal action of rising vapour bubbles and natural convection currents. The fluid plume thus generated drives a siphonic lateral fluid flow, which in turn changes the initial stagnant fluid medium at low heating levels to a more turbulent, almost forced convective type, boiling situation. These flow characteristics enhance the RB boiling cell heat transfer much above the convectional pool boiling and the single-phase RB cell thermal performance.

REFERENCES

[1] Hartmann. D.L., Moy. L.A., Fu. Q., Tropical convection and the energy balance at the top of the atmosphere, *Journal of Climate*, (2001) vol.14, pp. 4495–4511.

[2] Rahmstorf. S., The thermohaline ocean circulation: a system with dangerous thresholds, *Journal of Climate Change*, (2000), vol.46, pp. 247–256.

[3] Rajaram Lakkaraju, Boiling turbulent Rayleigh-Bénard convection, *PhD Thesis, (2012), University of Twente, Netherlands.*

[4] Podowski. R. M., Drew. D. A., Lahey. R. T., Podowski. J.R and M. Z., A mechanistic model of ebullition cycle in forced convection subcolled boiling, *8th international topical meeting on nuclear reactor thermal hydraulic*, (1997), Kyoto, Japan, 30 Sep-5 Oct, Proceeding Volume 3.

[5] Kurul, N., Podowski, M. Z., 1990. Multidimensional Effects in Forced Convection Subcooled Boiling, 9th International Heat Trans Conference. Jerusalem. Israel, Proceedings.

[6] Koncar, B., Kljenak, I., Mavko, B., 2004. Modelling of local two-phase flow parameters in upward subcooled flow boiling at low pressure. Int J Heat and Mass Trans. 47, 1499–1513.

[7] Krepper, E., Koncar, B., Egorov, Y., 2007. CFD modelling of subcooled boiling-Concept, validation and application to fuel assembly design. Nuclear Engineering and Design. 237, 716–731.

[8] Cole, R., 1960. A photographic study of pool boiling in the region of the critical heat flux, AIChE J, 6-4, 533–538.

[9] Lemmert, M., Chawla, L.M., 1977. Influence of flow velocity on surface boiling heat transfer coefficient in Heat Transfer in boiling. Academic Press and Hemisphere, NY, USA.

[10] Tolubinski., V.I., Kostanchuk, D.M., 1970. Vapour bubbles growth rate and heat transfer intensity at subcooled water boiling., 4th International Heat Transfer Conference, Paris, France.

[11] Ishii, M., Zuber, N., 1979. Drag coefficient and relative velocity in bubbly, droplet or particulate flows, AlChE J. 25-5, 843-855.

[12] Unal, H.C., 1979. Maximum Bubble diameter, maximum bubble growth time and bubble growth rate during subcooled nucleate flow boiling of water up to 17.7MN/m2. Int J. Heat and Mass Trans, 19, 643-649.

[13] Kataoka, I., Ishii, M., Mishima, K., 1983. Generation and size distribution of deoplet in annular two-phase flow, ASME J. Fluid Engineering. 105, 230-238.

[14] Moraga, F.J. Bonetto, F.J., Lahey, R.T., 1999. Lateral forces on spheres in turbulent uniform shear flow. Int J. Multiphase Flow 25, 1321-1372.

[15] De Bertodano, M.L., 1991. Turbulent bubbly flow in a triangular duct. Ph.D. Thesis, Rensselaer Polytechnic Institute, New York.

[16] Sato, Y., Sadatomi, M., 1981. Momentum and heat transfer in two-phase bubble flow - I. Theory, Int J. Multiphase Flow. 7-2, 167–177.

[17] Hosokawa, S., Tomiyama, A., Misaki, S., Hamada, T., 2002. Lateral migration of single bubbles due to the presence of wall, ASME Joint U.S.-European Fluids Engineering Division Conference, Montrea, Canada.

[18] Ranz, W.E., Marshall, W.R., 1952. Evaporation from drops. Parts I & II. Chem. Eng.. 48,141-6; 173-180.

[19] Kutateladze, S.S., 1950., Hydromechanical model of the crisis of boiling under conditions of free convection, Journal of Technical Physics, USSR 20 (11), 1389–1392.